

Numerical investigation of flow and heat transfer in a channel with different configurations and alternately order obstacles

<https://doi.org/10.32792/utq/utj/vol13/1/5>

Hayder Abdulhasan Lafta

Mechanical Engineering Department

College of Engineering – University of Thi qar

Haider_abdalhassan@utq.edu.iq

Abstract

In the present study, a numerical investigation has been made to predict the laminar flow and heat transfer through a rectangular channel with adiabatic, different configuration obstacles which are arranged alternately on the upper and lower walls of the channel. These walls are subjected to a constant heat flux 500 W/m^2 . The effect of obstacles number, and obstacles shape on the flow and heat transfer characteristics with different Reynolds number (100,200,300,400,500,600and 700) have been studied. The continuity, momentum, and energy governing equations are solved by the finite volume method. The results of this study reveal that the obstacles have an obvious effect on parameters of the flow and heat transfer enhancement. The heat transfer is improved more as the obstacle's number increase. Further that, using rectangular obstacle leads to increase heat transfer rate higher than the rest of shapes for all Reynolds number tested.

1. Introduction

Improvement of a single phase heat transfer channels depends on many techniques. One of these techniques includes finding vortex generator obstacles such as baffles, blocks, and ribs, in the path of flow. The presence of obstacles increases fluid mixing, recirculation, and reattachment to interrupt the hydrodynamics and thermal boundary layers, especially when these obstacles are arranged in a staggered manner where the flow will deflect and impinge the opposite walls. Consecutive interruption of boundary layers causes overall heat transfer improvement.

The geometrical characteristics of these obstacles play an important role in the rate of heat transfers. This way of heat transfer improvement is commonly used in many engineering applications such as; air cooled solar collectors, shell and tube heat exchangers, internally cooled turbine blades, cooling of electronic devices, and chemical catalytic reactors.

The first pioneer work of numerical investigation of fluid flow and heat transfer characteristics in a smooth channel with staggered baffles based on the periodically fully developed flow conditions was conducted by Patankar et al. [1]. The heat transfer in channels with staggered baffles was computed by Kelkar and Patankar [2], they found that the heat transfer increasing with the rise in baffle height and with the decrease in baffle spacing. Their obtained results showed agreement with results of Webb and Ramadhyani [3]. Miranda and Anand [4] studied numerically laminar forced convective heat transfer in a two dimensional parallel plate channel with (solid and porous) baffles mounted alternately on bottom and top walls. The channel walls were exposed to a constant heat flux condition. They found that the heat transfer enhancement ratio for solid-baffle cases are higher than those for corresponding porous-baffle cases, and the heat transfer enhancement ratio increased with increase in Reynolds number. A finite volume technique is used by Yang and Hwang [5] to investigate turbulent flow in a rectangular channel with staggered (solid and porous) baffles. The channel walls were maintained at a constant temperature condition on both upper and lower walls, eight baffles were put in a staggered manner. They showed that the heat transfer is enhanced with both solid and porous baffles compared to the smooth channels. Korichi and Oufer [6] investigated numerically the flow field and heat transfer enhancement in a channel with three obstacles, two attached to the lower wall and one to the upper wall. The study showed that the heat transfer was enhanced particularly for the second obstacle when Reynold number was increased. In the other study, Korichi and Oufer [7] performed numerical simulation of fluid flow and heat transfer in a horizontal channel with periodically mounted obstacles on both upper and lower walls. They reported significant heat transfer enhancement between the fluid and the heated obstacles of up to 123.1% in Nusselt number when Reynolds number increases from 50 to 500, and 48.5% in Nusselt number when Reynolds number increases from 500 to 1000. On the other side, they observed that the obstacle attached on both walls have higher values of up to 141% in Nusselt number than that attained from these obstacles mounted only on one single wall of channel. Laminar flow

and heat transfer in a channel fitted with two transverse staggered diamond-shaped baffles was investigated by Sripattanapipat and Promvongse [8], the factor of interest was the half tip angle of diamond baffles which was varied in range of $\theta=5^\circ$ to $\theta=35^\circ$. They found that the thermal performance of the $5^\circ - 10^\circ$ diamond baffle is higher than that of the flat baffle for all Reynolds number used (100-600). Convective heat transfer over an array of obstacles of both rectangular and squared shapes was studied by Jubran et al [9]. They showed that the use of individual rectangular modules enhanced heat transfer more than the square modules did. A numerical study of the heat transfer behavior in the instance of a channel with baffles mounted in staggered manner with Reynolds number from 50 to 500 and baffle heights from 0 to 0.75 was conducted by Mousavi and Hooman [10], they observed that increasing the blockage ratio and Reynolds number will increase the Nusselt number. Parndtl number affects the precise location of the periodically fully developed region. Gareh [11] carried out numerical investigation of heat transfer in a rectangular channel with mounted obstacle. He showed that as the value of the Reynolds number increases, the heat removed from the obstacles increases sensibly with a maximum heat removal around the obstacle corners. Further that the vortex shedding generated by the obstacle on the lower wall can additionally enhance heat transfer along the obstacle surface. In another study, Gareh [12] found that a travelling wave generated by the vortex shedding contributes mainly to heat transfer enhancement.

The purpose of the present study is to investigate numerically the laminar flow and heat transfer in a rectangular, two dimension channel with adiabatic obstacles arranged alternately on the upper and lower wall of the channel. The obstacle shape and obstacle number are investigated with different values of Reynolds numbers to show how these obstacles with various characteristics can affect on the flow dynamics and heat transfer enhancement.

2. Model description

2.1. Mathematical model

In this study, the geometrical configuration is considered as shown in fig. (1). Two –different shapes– obstacles mounted on both upper and lower walls of channel in a staggered manner. The flow is considered laminar, incompressible and two dimensional. The physical properties of fluid and solid are assumed constant. A constant heat flux is applied on

both upper and lower walls of channel. The fluid flow is fully developed and enters the channel in velocity with a parabolic profile. The computation domain is divided into three region, inlet region where ($x=0$ to $x=l_1$), the inlet region length (l_1) is assumed 6 times of the height of channel, the obstacle region where ($x=l_1$ to $x=L-l_2$), and the outlet region where ($x=L-l_2$ to $x=L$), the outlet region length (l_2) is assumed 14 times of the height of channel to prevent any elliptic effects at the channel exit [13]. The length of each shape of obstacles depends on the assumed width with constant face area for all shapes.

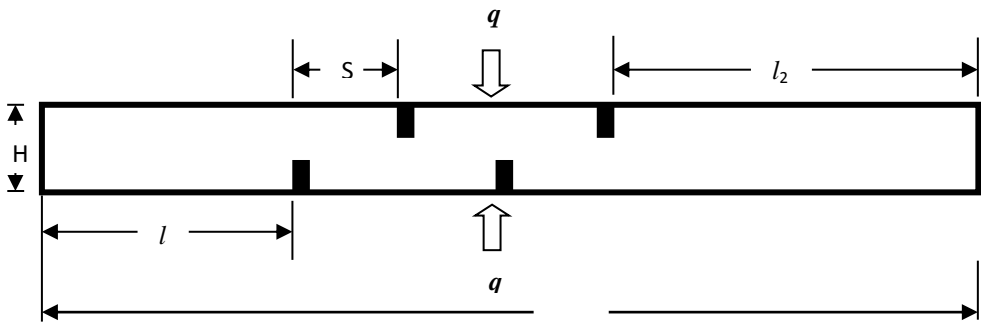


Fig.(1) Channel geometry

The governing equations of continuity, momentum and energy are presented in the Cartesian coordinate system and can be written as:

Continuity equation

$$\frac{\partial u}{\partial x} + \frac{\partial v}{\partial y} = 0 \quad (1)$$

x-momentum equation:

$$\frac{\partial u}{\partial t} + u \frac{\partial u}{\partial x} + v \frac{\partial u}{\partial y} = -\frac{\partial p}{\partial x} + \frac{1}{Re} \left(\frac{\partial^2 u}{\partial x^2} + \frac{\partial^2 u}{\partial y^2} \right) \quad (2)$$

y-momentum equation:

$$\frac{\partial v}{\partial t} + u \frac{\partial v}{\partial x} + v \frac{\partial v}{\partial y} = -\frac{\partial p}{\partial y} + \frac{1}{Re} \left(\frac{\partial^2 v}{\partial x^2} + \frac{\partial^2 v}{\partial y^2} \right) \quad (3)$$

Energy equation:

$$\frac{\partial T}{\partial t} + u \frac{\partial T}{\partial x} + v \frac{\partial T}{\partial y} = \frac{1}{Pr} \left(\frac{\partial^2 T}{\partial x^2} + \frac{\partial^2 T}{\partial y^2} \right) \quad (4)$$

The parameters of this study are: Reynolds number, friction factor and Nusselt number.

The Reynolds number is defined as:

$$Re = \frac{\rho u D_H}{\mu} \quad (5)$$

The friction factor is computed by pressure drop (ΔP) across the length of the channel L as:

$$f = \frac{\Delta P}{1/2 \rho U^2} \frac{D_H}{L} \quad (6)$$

The heat transfer is measured by the local Nusselt number along the lower and upper walls of the channel as:

$$Nu = \frac{h D_H}{k} \quad (7)$$

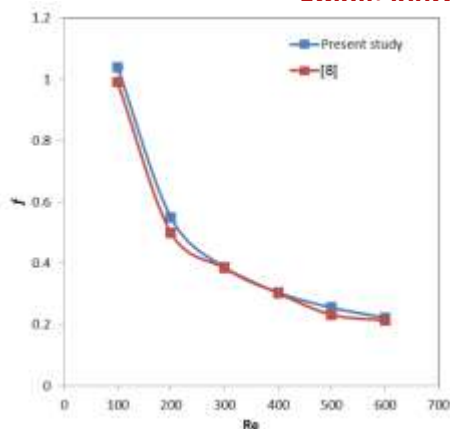
Where $h = \frac{q}{A(T_w - T_b)}$

The average Nusselt number for the lower and upper walls of the channel is calculated as:

$$Nu_{av} = \frac{Nu_{lower} + Nu_{upper}}{2}$$

2.2. Boundary conditions

The fluid flow at inlet channel is assumed fully developed with parabolic profile $u(y) = 6u_o(y/H)[1 - (y/H)]$. For the channel's upper and lower walls and the obstacles, no-slip wall condition ($y = 0$ and $y = H, u = v = 0$) are applied. The inlet air temperature is equal to 300°k, ($Pr = 0.7$) and constant physical properties of the air. At the upper and lower walls, constant heat flux condition was applied with 500 W/m². The obstacle walls are considered as adiabatic. The face area of obstacles is (20 cm²) for four shapes (square, rectangular, triangle, and hemi circle) were considered. The obstacles spacing (S/H) is fixed and equal to 1.



equations associated with boundary y solved using the finite volume hm of Pantankar [14] has been used. nuous until the residual for all n 10^{-6} for all dependent variables.

tested by applying different, uniform Re=500, area of face of obstacle =20 ectangular shape. Table 1 represents a less than 3.2×10^{-3} change in Nu when the grid element number is increased to 23228. Therefore the grid element number of 16362 has been chosen in present work.

Grid element no.	Nu_{Av}
3977	12.1948
9164	12.4221
16362	12.5134
23228	12.5536

Table 1: Effect of grid refinement on the average Nusselt number

3. Verification

Verification of the heat transfer and friction factor of the smooth channel without obstacles is performed by comparing the present study with [8] under a similar condition as shown in Fig.(2) and Fig.(3) respectively.

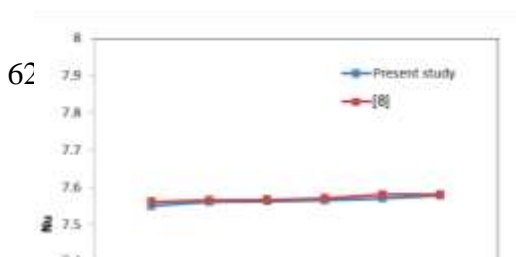


Fig. (2) Verification of friction factor of [8] with present study

Fig.(3) Verification of Nusselt number of [8] with present study.

The verification results are found to be in excellent agreement with [8] for both the Nusselt number and friction factor. This provides a strong confidence in further investigation of the channel flow over the obstacles.

4. Results and discussions

The obtained results for a rectangular channel, incompressible laminar flow with different geometric configuration obstacles are discussed below. Effects of number of obstacles, shape of obstacles with different Reynolds number on the hydrodynamic and thermal field are studied.

4.1. Effects of obstacles number on the hydrodynamic flow and thermal domain

The effect of number of obstacle on the flow structure at specified Reynolds number is explained in fig (4). The stream function contours for the cases of no obstacle, one, and two obstacles on each wall are plotted in fig (4) respectively. Presence of obstacles causes interrupt of hydrodynamics boundary layer. The re-circulation zone downstream of the obstacles produced due to the fluid mixing, deflecting, and reattachment of the flow. Therefore, increasing number of obstacles causes increasing number of re-circulation area. The plot explains that the re-circulation zone develops to a long distance by adding one obstacle and it becomes longer with four re-circulation zones when adding two obstacles.

Fig. (5) Shows the variation of the friction factor ratio for cases of different number of obstacles. When number of obstacles increases, the

friction factor ratio increases due to increasing in the re-attachment, separation, and deflection zone.

Fig. (6) Represents the temperature distribution contours for different number of rectangular obstacles. It is obvious that the zone of high fluid temperature lie in the one obstacle and two obstacles cases. Presence of obstacles produces to increase the mixing and reattaching fluid which due to create reverse flow. This action will cause to deflect and impinge over the opposite walls of channel leading to increasing heat losses.

Fig. (7) Shows the variation of the average Nusselt number with Reynolds number for different numbers of the rectangular obstacles. As the obstacle number increases, the average Nusselt number increases. The increasing in the average Nusselt number is due to the intense mixing fluid by the induced vortex.

Fig. (8) Shows the variation of pressure drop with Reynolds number for different number of rectangular obstacles. It can be seen that the pressure drop increases as the number of obstacles and Reynolds number increases respectively. Presence of obstacles dues to increase the re-attachment zones which produces friction higher than other zones across the channel. This trend arise the drop pressure as more as obstacles number increase.

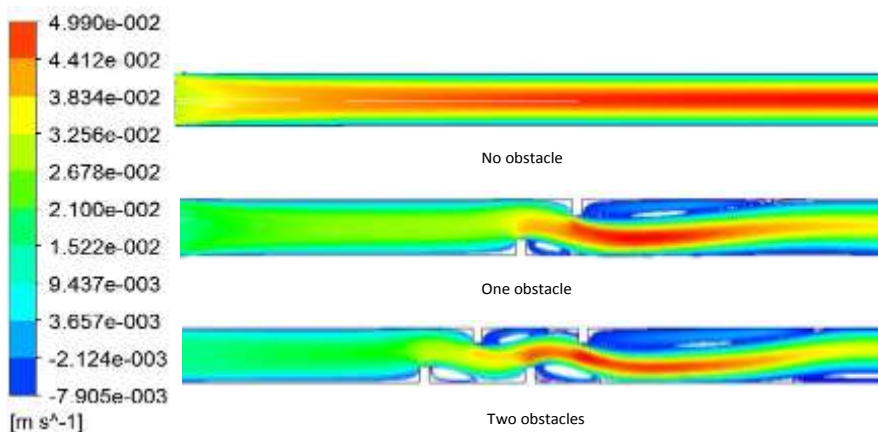


Fig. (4) Stream function contour for rectangular obstacle at Re=500.

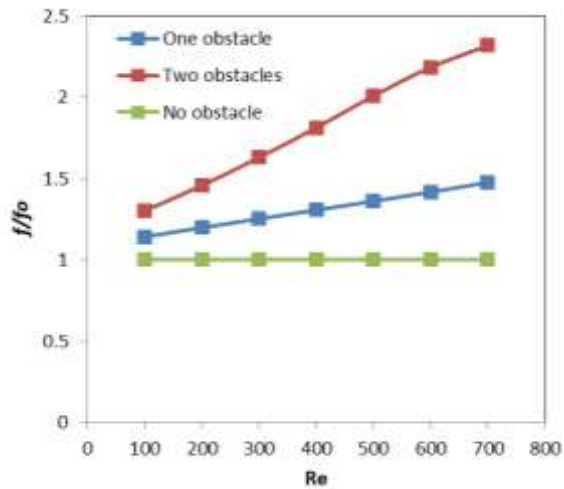


Fig. (5) Friction factor ratio with Reynolds number for rectangular obstacles at each side of the channel.

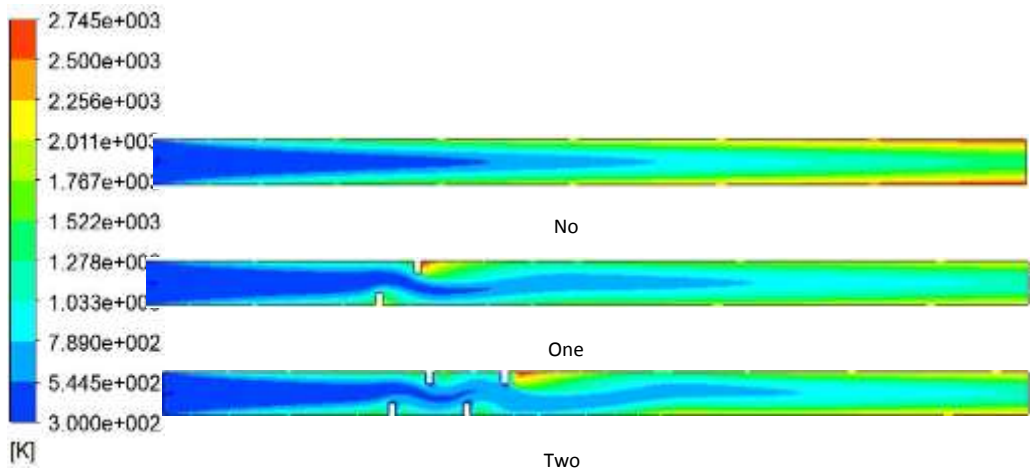


Fig. (6) Temperature distribution contours for rectangular obstacles at $Re=400$

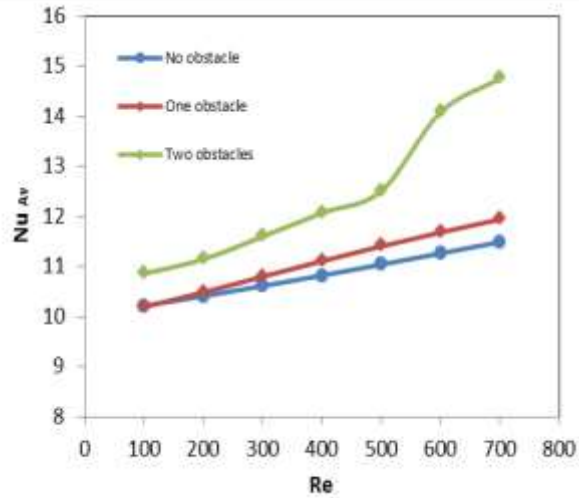


Fig.(7) Average Nusselt number with Reynolds number for different rectangular obstacle numbers

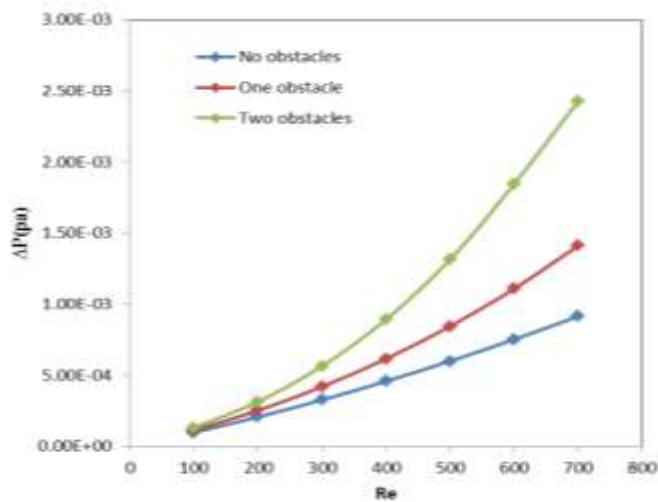


Fig. (8) Pressure drop with Reynolds number for different rectangular obstacle numbers.

4.2 Effects of obstacles shape on the hydrodynamic flow and thermal domain

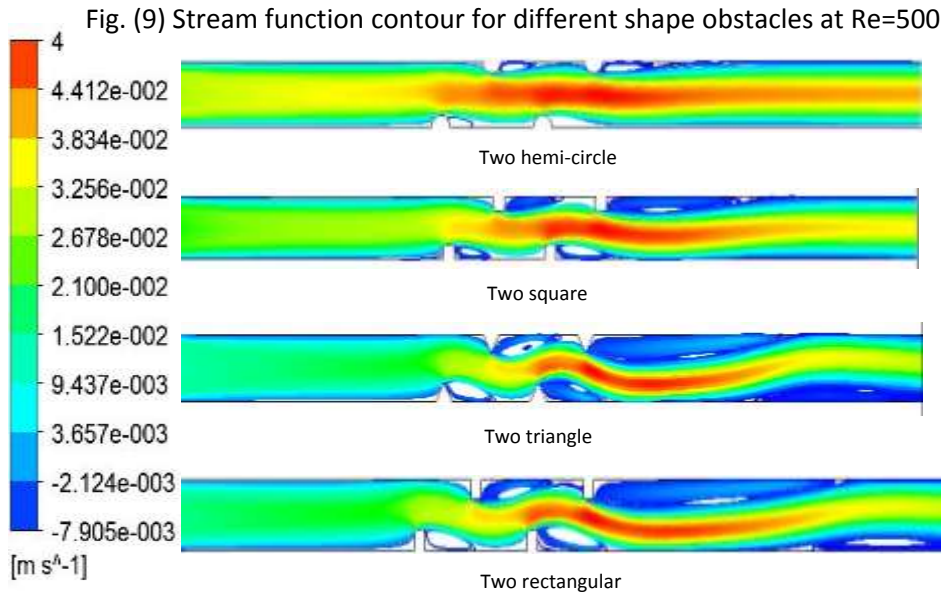
The effect of obstacles shape on the flow structure at specified Reynolds number is explained in fig. (9). The stream function contour for the cases of two hemi circle obstacles, two square obstacles, two triangle obstacles and two rectangular obstacles on each wall of channel are plotted in fig.(9) respectively. The effect of the obstacle shape on the stream function contour is observed that the length of re-circulation zone increasing as the obstacle shape change from hemi circle to square then to triangle and then to rectangular sequentially. The longer re-circulation zone is obtained where the rectangular obstacle is exist. This trend is produced because the rectangular obstacle has longer edge which faces the fluid flow than the other obstacles although all of the obstacles have the same face area (20 cm^2). That induces to increase the extension of re-circulation zone and washing action.

Fig. (10) Shows the variation of friction factor ratio for different shape of obstacles. As the shape is changing from the hemi circle to square the friction factor is increased. But for the triangle and rectangular shape, it can be seen that at low Reynolds number, the friction factor of rectangular is higher than the triangular until the $Re=400$ where they are equal. After that the triangle obstacle becomes higher than the rectangular obstacle because the geometry of the shape of obstacles and hydrodynamic characteristics.

Fig. (11) Shows the temperature distribution contours for different shapes of obstacles. It is clear that the zone of high fluid temperature is growing from the hemi circle obstacle case to square obstacle case and then got more at triangle obstacle until reached the maximum at the rectangular obstacle case because the rectangular obstacles produce bigger re-circulation and reattachment zones due to increase the mixing fluid and heat losses.

Fig. (12) Explains the effect of the obstacle shape on the Nusselt number. It is found that as the obstacle shape changing from hemi circle shape to square shape and to triangle shape the Nusselt number increases until reached the higher value at the rectangular shape obstacle for all Reynolds number cases. The recirculation zone is graduated in growth from the hemi circle shape to rectangular shape which the mixing and vortex will be greater.

Fig. (13) Shows the variation of pressure drop with Reynolds numbers for different shape of obstacles. It can be seen that the pressure drop is increasing from the hemi circle shape until reached the highest value at the triangle shape which is the friction factor is the highest.



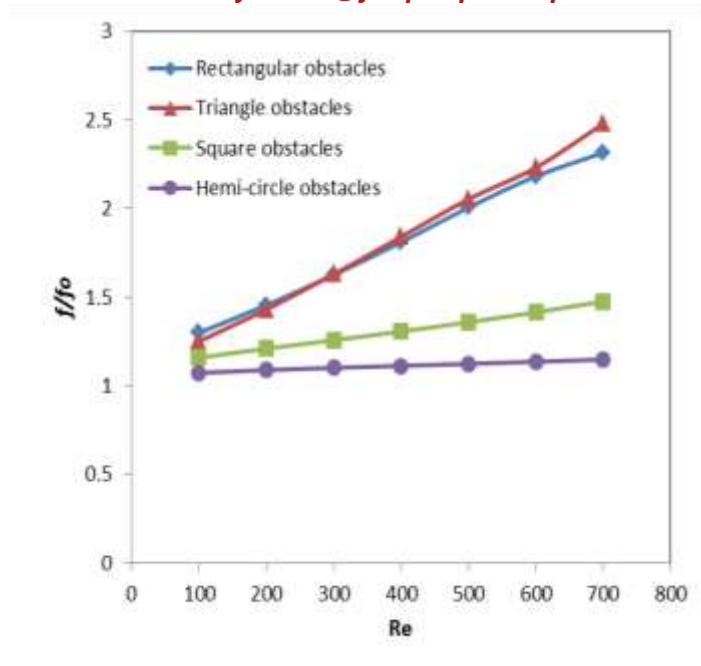


Fig. (10) Friction factor ration with Reynolds number for different shapes of obstacles

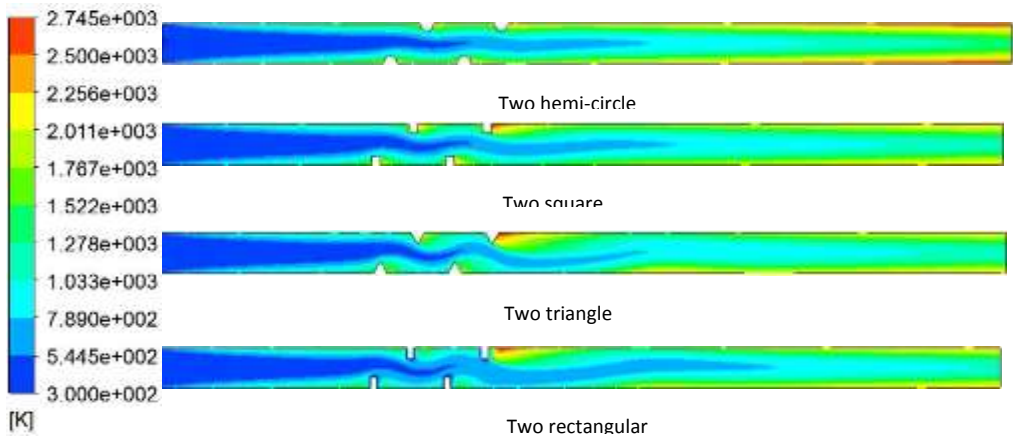


Fig. (11) Temperature distribution contours for different obstacle

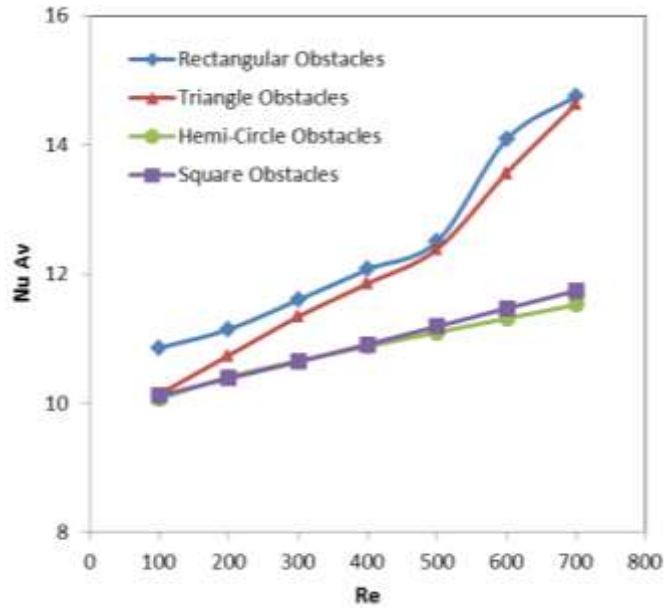


Fig. (12) Average Nusselt number with Reynolds number for different shapes of obstacles.

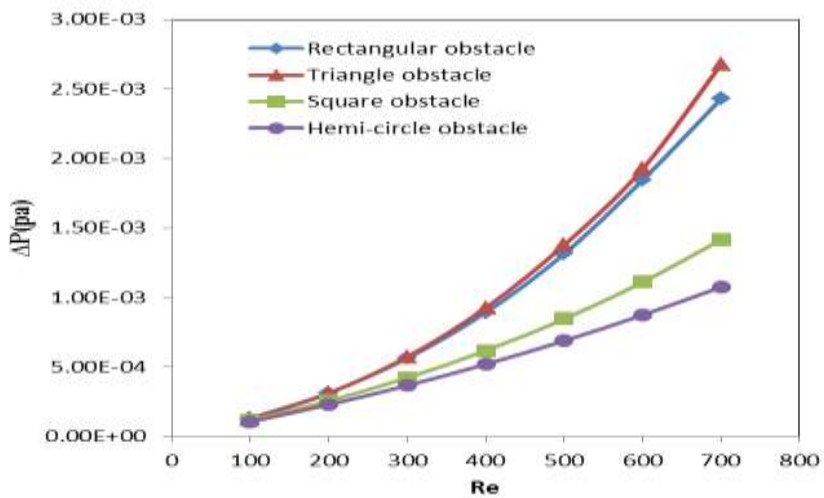


Fig. (13) Pressure drop with Reynolds number for different shapes of obstacles.

5. Conclusions

The results are presented for a fixed baffles spacing ($S/H=1.0$), different shapes, numbers, and Reynolds number (100,200,300,400,500,600, and 700). Conclusions can be summarized as below:

- Presence of obstacles in a channel in staggered manner increases the rate of heat transfer by considerable value.
- Increasing number of obstacles leads to increase the rate of heat transfer and the friction factor ratio.
- Nusselt number is increased as Reynolds number increased for all cases.
- The drop pressure increases as Reynolds number increased for all cases.
- Changing the obstacle shapes from the hemi circle shape to square shape to triangle shape reaching to rectangular shape seemed to increase the heat transfer rate where the higher heat transfer and Nusselt number are obtained at the rectangular obstacle shape.

6. Nomenclature

Symbol	Description
ΔP	Pressure drop, Pa.
μ	Kinematic viscosity, $\text{kg s}^{-1} \text{m}^{-1}$.
D_H	Hydraulic diameter ($=2H$), m.
f	Friction factor
f_o	Friction factor at smooth channel
H	Height of channel, m.
h	Heat transfer coefficient, $\text{W m}^{-2} \text{K}^{-1}$.
K	Thermal conductivity, $\text{W m}^{-1} \text{k}^{-1}$.
L	Length of channel, m.
l_1	Length of entrance region, m.
L_f	Length of exit region, m.

Nu_{AV}	Average Nusselt number
Pr	Prandtl number
q	Heat flux, Wm ⁻² .
Re	Reynolds number
S	Space between obstacles, m.
Tb	Bulk temperature, K.
Tw	Wall temperature, K.
u	Velocity, m.
ρ	Density, kg m ⁻³ .

References

1. Patankar, S. V., C. H. Liu, and E. M. Sparrow. "Fully developed flow and heat transfer in ducts having streamwise-periodic variations of cross-sectional area." *ASME J. Heat Transfer* 99.2 (1977): 180-186.
2. Kelkar, K. Mt, and S. V. Patankar. "Numerical prediction of flow and heat transfer in a parallel plate channel with staggered fins." *Journal of heat transfer* 109.1 (1987): 25-30.
3. Webb, B. W., and S. Ramadhyani. "Conjugate heat transfer in a channel with staggered ribs." *International Journal of Heat and Mass Transfer* 28.9 (1985): 1679-1687.
4. Da Silva Miranda, Bruno Monte, and N. K. Anand. "Convective heat transfer in a channel with porous baffles." *Numerical Heat Transfer, Part A: Applications* 46.5 (2004): 425-452.
5. Yang, Yue-Tzu, and Chih-Zong Hwang. "Calculation of turbulent flow and heat transfer in a porous-baffled channel." *International Journal of Heat and Mass Transfer* 46.5 (2003): 771-780.
6. Korichi, Abdelkader, and Lounes Oufier. "Numerical heat transfer in a rectangular channel with mounted obstacles on upper and lower walls." *International Journal of Thermal Sciences* 44.7 (2005): 644-655.

7. Korichi, Abdelkader, and Lounes Oufer. "Heat transfer enhancement in oscillatory flow in channel with periodically upper and lower walls mounted obstacles." *International Journal of Heat and fluid flow* 28.5 (2007): 1003-1012.
8. Sripattanapipat, Somchai, and Pongjet Promvonge. "Numerical analysis of laminar heat transfer in a channel with diamond-shaped baffles." *International Communications in Heat and Mass Transfer* 36.1 (2009): 32-38.
9. Jubran, B. A., S. A. Swiety, and M. A. Hamdan. "Convective heat transfer and pressure drop characteristics of various array configurations to simulate the cooling of electronic modules." *International Journal of Heat and Mass Transfer* 39.16 (1996): 3519-3529.
10. Mousavi, Saman S., and Kamel Hooman. "Heat and fluid flow in entrance region of a channel with staggered baffles." *Energy Conversion and Management* 47.15 (2006): 2011-2019.
11. Gareh, Salim. "Numerical heat transfer in a rectangular channel with mounted obstacle." *International Letters of Chemistry, Physics and Astronomy* 19.2 (2014): 111-119.
12. Gareh, Salim. "Numerical steady of laminar flow over two-dimensional obstacle." (2014).
13. Mushatet, Khudheyer S., Qais A. Rishakb, and Mohsen H. Fagr. "Numerical study of laminar flow in a sudden expansion obstructed channel." *Thermal Science* 19.2 (2015): 657-668.
14. Patankar, Suhas. *Numerical heat transfer and fluid flow*. CRC press, 1980.